

BSSRDF Estimation from Single Images.

Adolfo Munoz¹ Jose I. Echevarria¹ Francisco J. Seron¹ Jorge Lopez-Moreno¹ Mashhuda Glencross² Diego Gutierrez¹
¹Universidad de Zaragoza ²Loughborough University

Supplementary Material

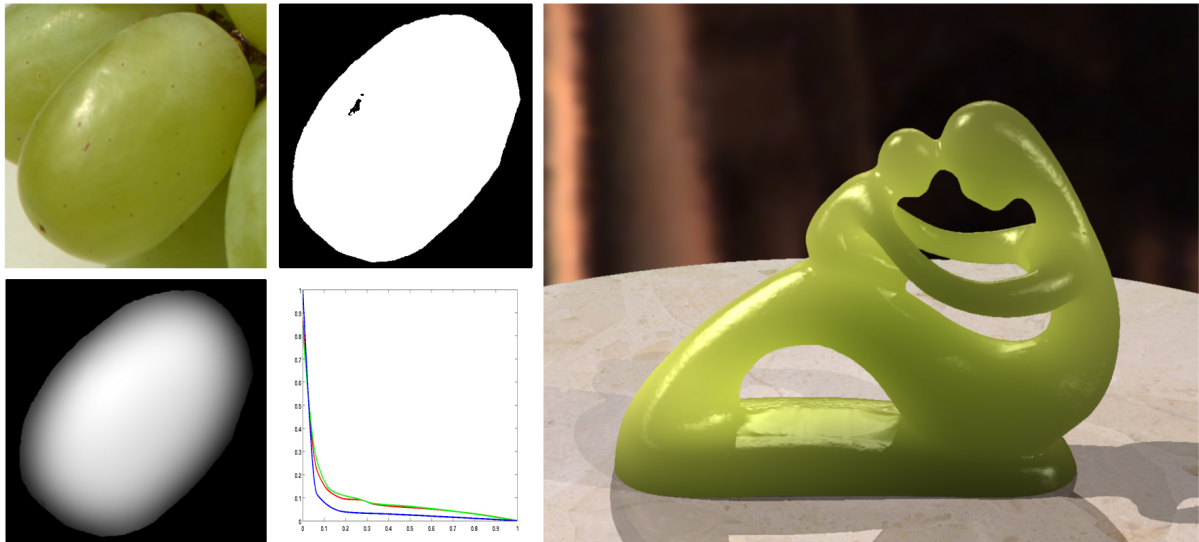


Figure 1: Capture and rendering of a grape: *Photograph, Matte, Depthmap, Profile and rendered image*

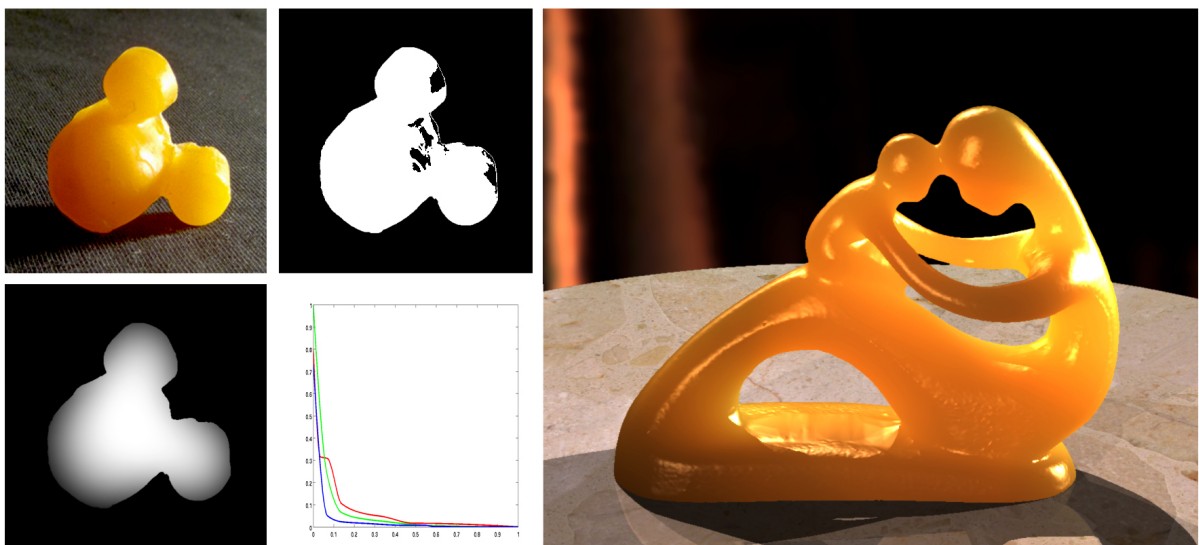


Figure 2: Capture and rendering of orange soap: *Photograph, Matte, Depthmap, Profile and rendered image*

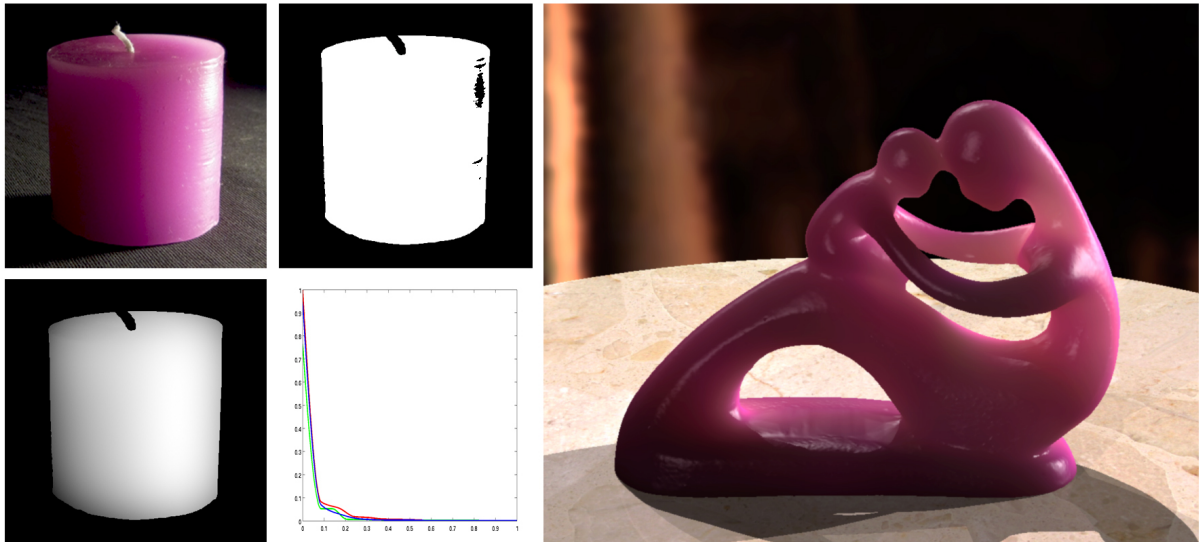


Figure 3: Capture and rendering of a wax candle: Photograph, Matte, Depthmap, Profile and rendered image

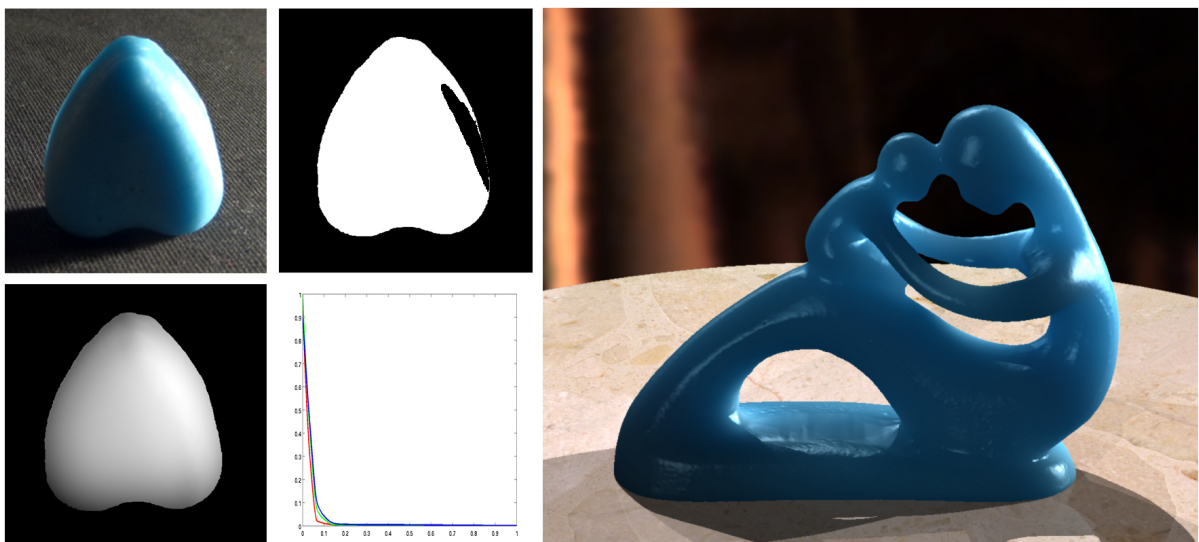


Figure 4: Capture and rendering of blue soap: Photograph, Matte, Depthmap, Profile and rendered image

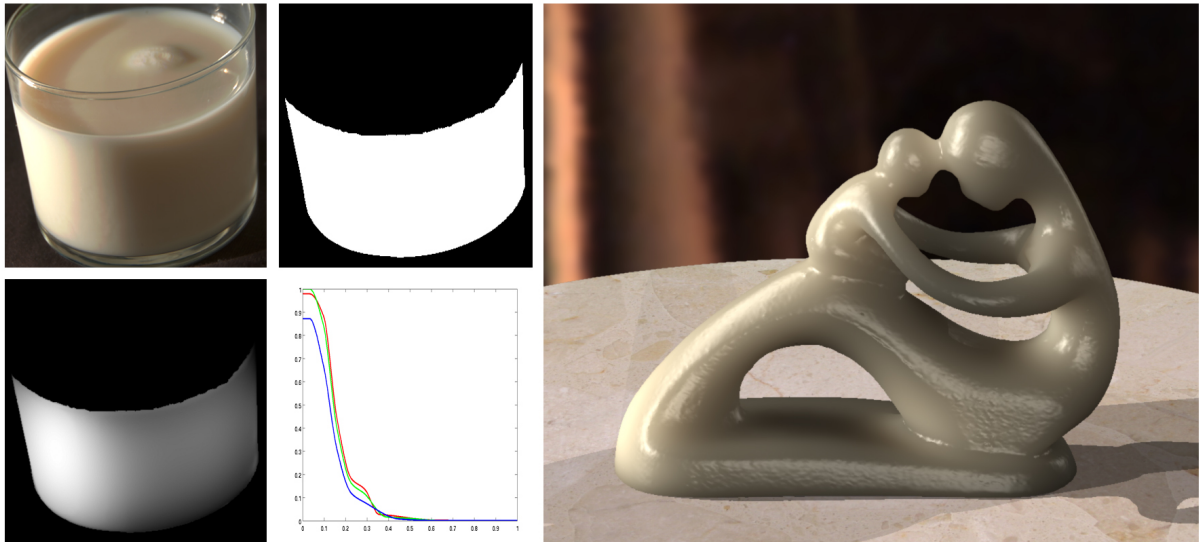


Figure 5: Capture and rendering of whole milk: Photograph, Matte, Depthmap, Profile and rendered image

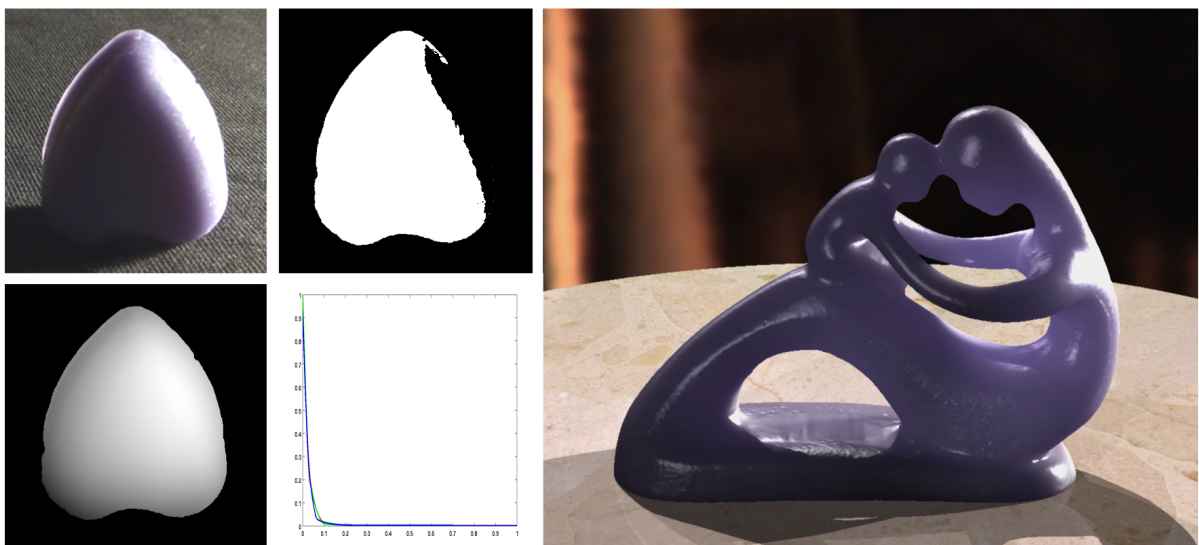


Figure 6: Capture and rendering of purple soap: Photograph, Matte, Depthmap, Profile and rendered image

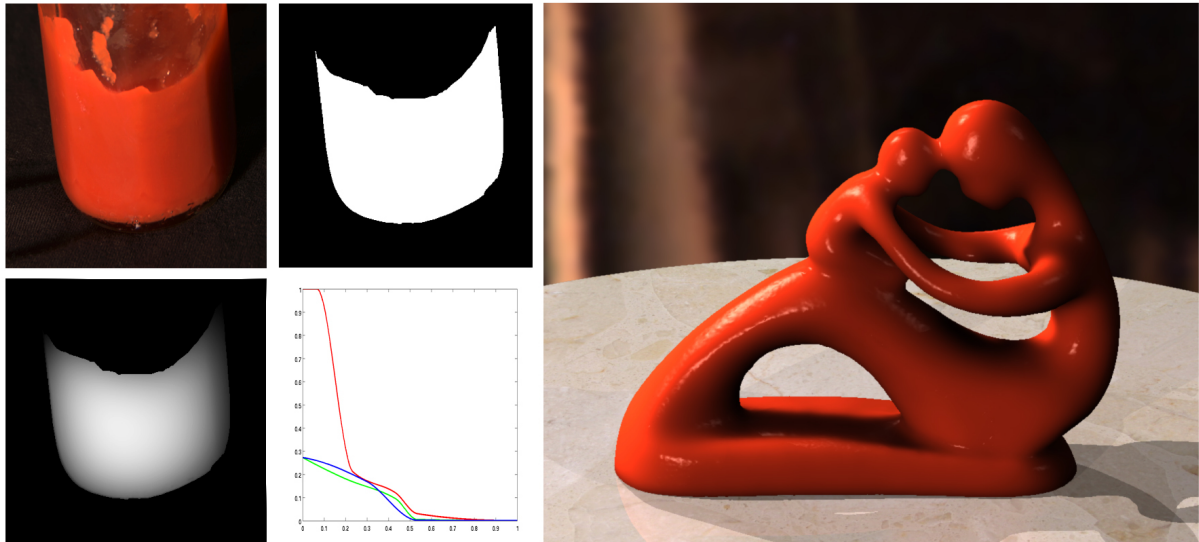


Figure 7: Capture and rendering of ketchup sauce: Photograph, Matte, Depthmap, Profile and rendered image

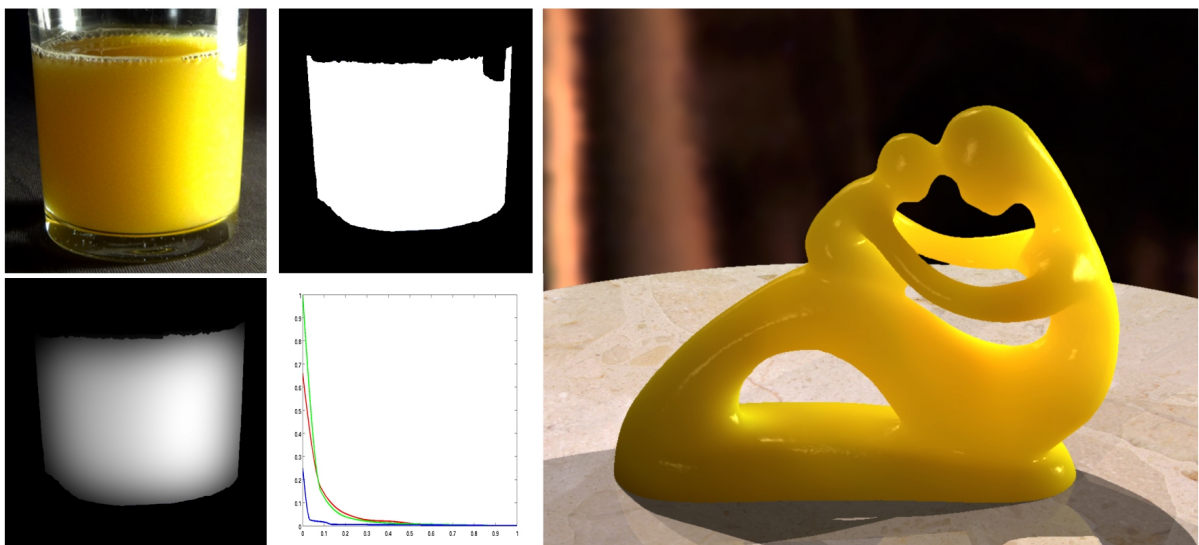


Figure 8: Capture and rendering of orange juice: Photograph, Matte, Depthmap, Profile and rendered image

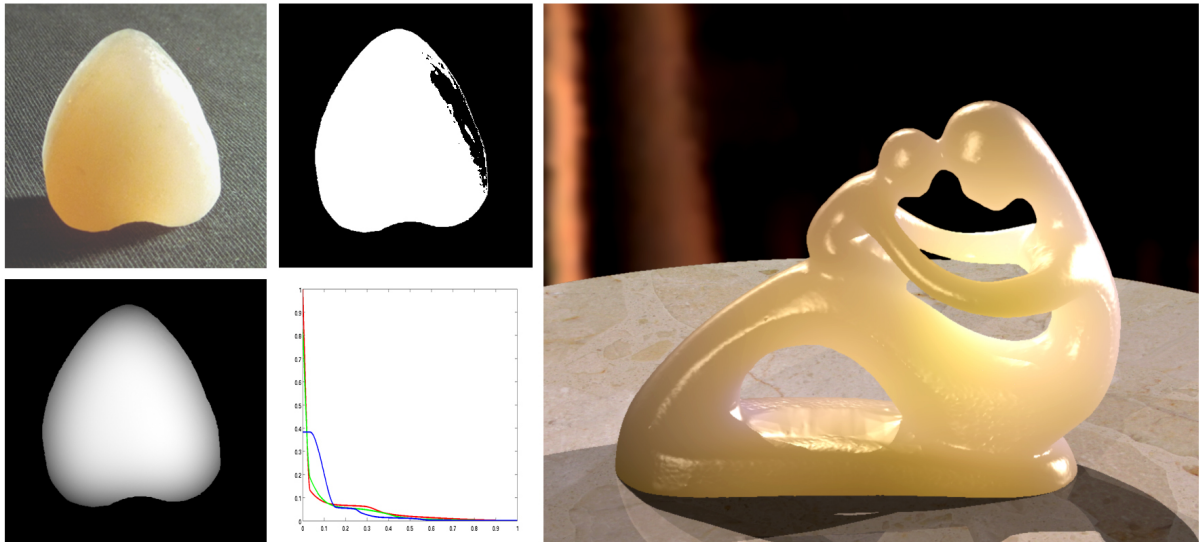


Figure 9: Capture and rendering of whitish soap: Photograph, Matte, Depthmap, Profile and rendered image

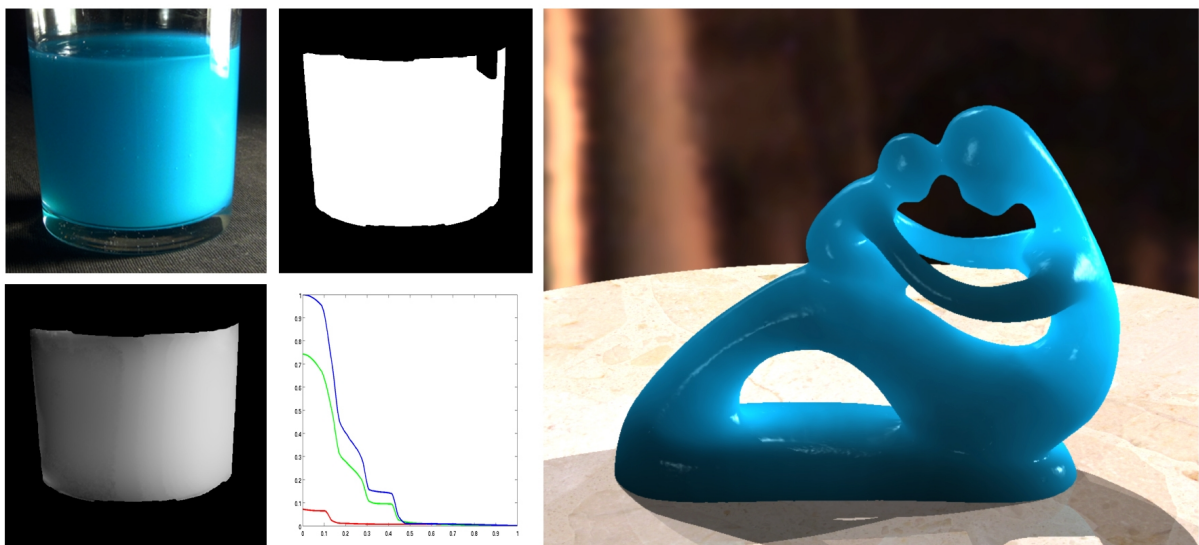


Figure 10: Capture and rendering of liquid detergent: Photograph, Matte, Depthmap, Profile and rendered image

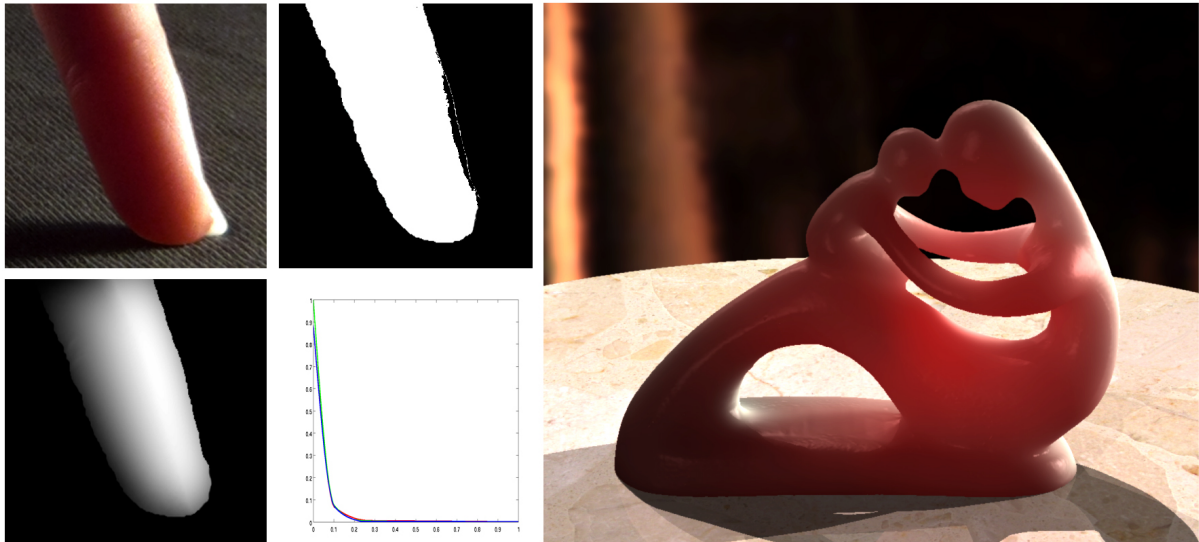


Figure 11: Capture and rendering of human skin: Photograph, Matte, Depthmap, Profile and rendered image

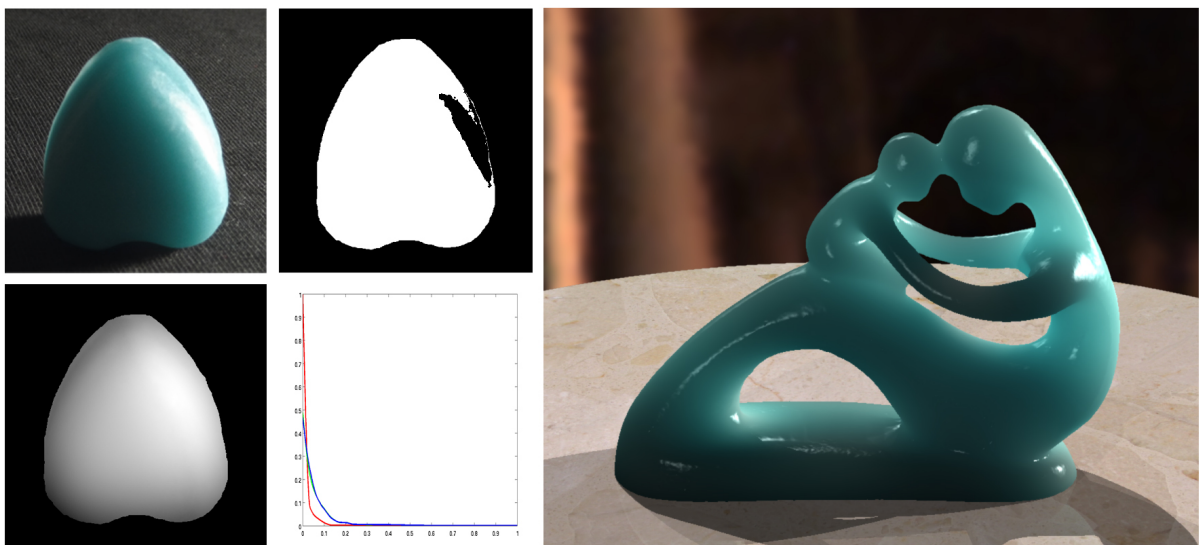


Figure 12: Capture and rendering of greenish soap: Photograph, Matte, Depthmap, Profile and rendered image

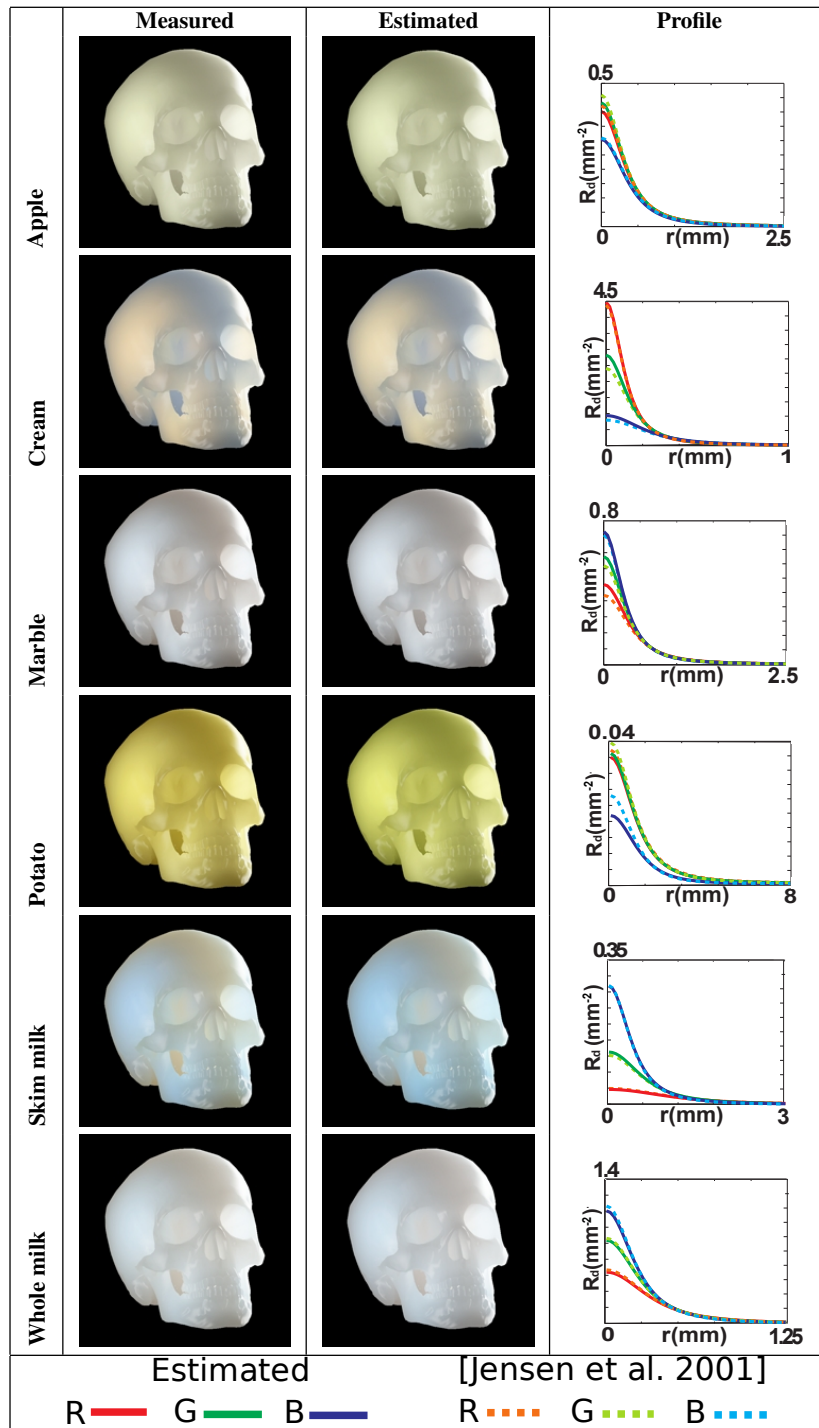


Figure 13: Left two columns: Comparison between renderers using materials from [Jensen et al. 2001] and our estimated diffusion profiles. Right column: Comparison of diffusion profiles.









	Extruded matte	Base layer	Base and detail	3D	Ground truth
Depth map					
Result	Does not converge				

Figure 14: Top: results of different depth estimation techniques of increasing complexity, including ground-truth 3D data. Bottom: results of our method for the estimated profiles of the whole milk material, using the different depth maps (source shown at the right-most image). It can be seen how the simplest method does not converge, whereas using only a base layer may lead to unsatisfactory results. A good balance between visual accuracy and simplicity is better achieved with the combination of base and detail layers, yielding results very similar to using the true depth.

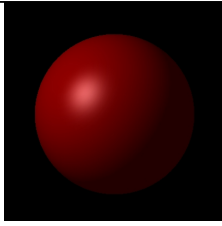
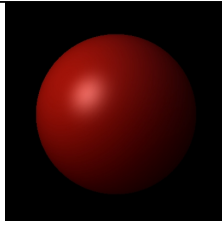
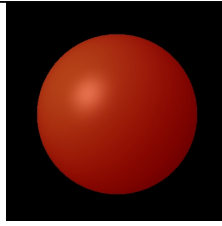
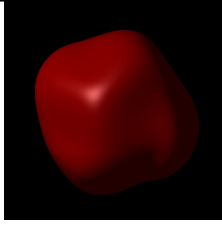
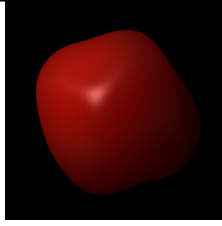
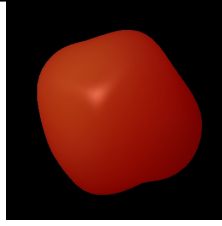
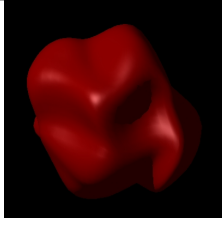
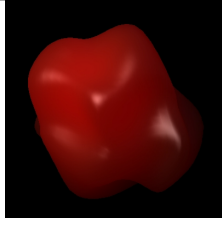
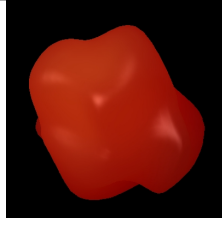
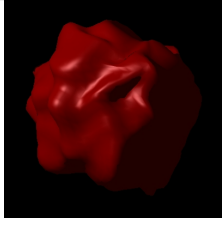
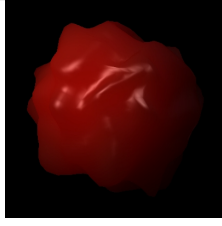
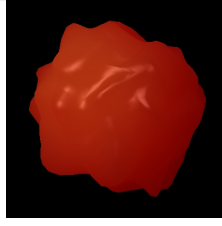
	Opaque		Translucent		Very translucent	
Geometry 1						
	θ	ϕ	θ	ϕ	θ	ϕ
	145.0°	52.1°	142.0°	51.0°	142.7°	50.5°
Error	0.0°	7.1°	-3.0°	6.0°	-2.3°	5.5°
Geometry 2						
	θ	ϕ	θ	ϕ	θ	ϕ
	152.5°	60.5°	149.9°	60.1°	156.2°	52.5°
Error	7.5°	15.5°	4.9°	15.1°	11.2°	7.5°
Geometry 3						
	θ	ϕ	θ	ϕ	θ	ϕ
	155.3°	61.3°	149.9°	60.1°	154.3°	59.8°
Error	10.3°	16.3°	4.9°	15.1°	9.3°	14.8°
Geometry 4						
	θ	ϕ	θ	ϕ	θ	ϕ
	159.2°	50.3°	149.0°	51.8°	153.4°	56.9°
Error	14.2°	5.3°	4.0°	6.8°	8.4°	11.9°

Figure 15: Performance of the light detection method for objects with varying degrees of translucency and geometric complexity. The images have been rendered with a directional light source at $(\theta, \phi) = (145^\circ, 45^\circ)$. The results of the light detection algorithm are shown under each image, along with the relative error. The error is always $\epsilon < 20^\circ$, which is below perceptual threshold.

	Opaque		Translucent		Very translucent	
Light (0, 0)						
	θ	ϕ	θ	ϕ	θ	ϕ
	11.85°	8.63°	-9.75°	2.79°	-10.71°	2.61°
Error	11.85°	8.63°	9.75°	2.79°	10.71°	2.61°
Light (0, 35)						
	θ	ϕ	θ	ϕ	θ	ϕ
	-11.84°	33.17°	-11.84°	36.62°	-11.84°	43.02°
Error	11.84°	1.83°	11.84°	1.62°	11.84°	8.02°
Light (0, 70)						
	θ	ϕ	θ	ϕ	θ	ϕ
	-13.97°	68.33°	-17.30°	72.77°	-12.84°	81.53°
Error	13.97°	1.67°	17.30°	2.77°	12.84°	11.53°
Light (120, 0)						
	θ	ϕ	θ	ϕ	θ	ϕ
	122.62°	22.57°	120.96°	20.60°	120.11°	12.84°
Error	2.62°	22.57°	0.96°	20.60°	0.11°	12.84°
Light (120, 35)						
	θ	ϕ	θ	ϕ	θ	ϕ
	120.96°	35.59°	123.42°	33.78°	124.99°	34.73°
Error	0.96°	0.59°	3.42°	1.22°	4.99°	0.27°

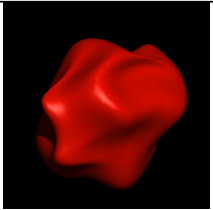
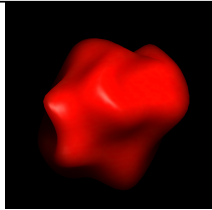
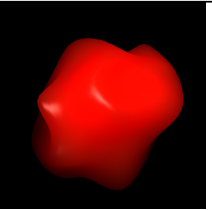
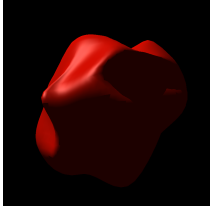
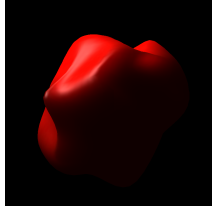
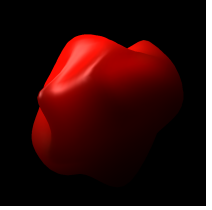

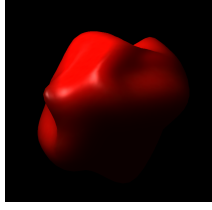
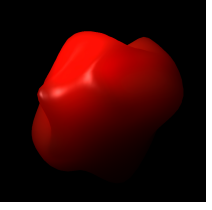
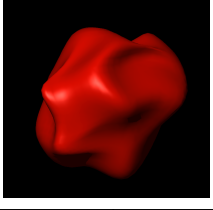
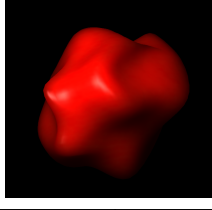
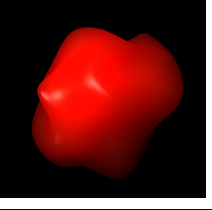
	Opaque		Translucent		Very translucent	
Light (120, 70)						
	θ	ϕ	θ	ϕ	θ	ϕ
	123.42°	59.55°	120.96°	63.81°	93.43°	71.81°
Error	3.42°	10.45°	0.96°	6.19°	26.57°	1.81°
Light (60, 0)						
	θ	ϕ	θ	ϕ	θ	ϕ
	56.58°	21.38°	57.38°	10.47°	61.63°	8.92°
Error	3.42°	21.38°	2.62°	10.47°	1.63°	8.92°
Light (60, 35)						
	θ	ϕ	θ	ϕ	θ	ϕ
	55.78°	23.59°	56.58°	23.30°	60.75°	24.45°
Error	4.22°	11.41°	3.42°	11.70°	0.75°	10.55°
Light (60, 70)						
	θ	ϕ	θ	ϕ	θ	ϕ
	54.25°	57.51°	55.01°	60.81°	59.63°	65.71°
Error	5.75°	12.49°	4.99°	9.19°	0.37°	4.29°

Figure 16: Performance of the light detection method for an object with varying degrees of translucency and different light directions. The images have been rendered with a directional light source at the specified (θ, ϕ) directions. The results of the light detection algorithm are shown under each image, along with the error. For translucent materials, the error is always $\epsilon < 20^\circ$, which is below perceptual threshold. An exception occurs in the case of $(\theta = 120^\circ, \phi = 0^\circ)$, for which the error in ϕ is 20.60° .

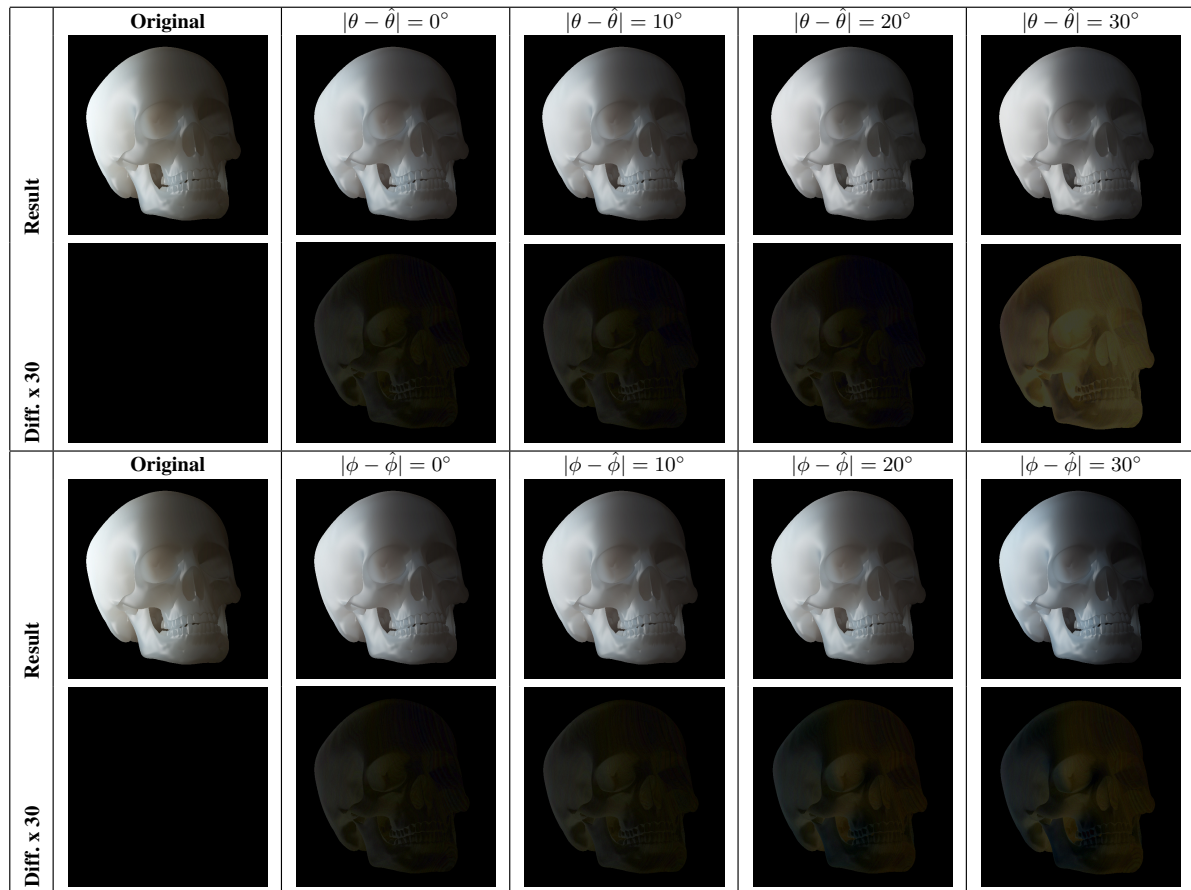


Figure 17: Behavior of the BSSRDF estimation algorithm according to the error on the light estimation (both on azimuth and zenith). The resulting renderings are visually accurate up to an error of 20° .